

Safranin-O Dye Removal from Aqueous Solution Using Superabsorbent Lignin Nanoparticle/Polyacrylic Acid Hydrogel

KH. Didehban^{1*}, S. A. Mirshokraie¹, J. Azimvand¹

¹ Department of Chemistry, Payame Noor University, Tehran, IRAN

Received 1 November 2017 • Revised 22 February 2018 • Accepted 21 March 2018

ABSTRACT

Alkali lignin (AL) modified by ethylene glycol and lignin nanoparticles (LN) was prepared through the acid precipitation technology. Lignin nanoparticle/polyacrylic acid (LN/PAA) hydrogel was prepared using copolymerization reactions. LN and LN/PAA hydrogel were investigated using GPC, SEM, FT-IR spectroscopy, and TGA-DTG analysis. The sizes of the nanoparticles were assessed using DLS. LN/PAA hydrogel was used to remove Safranin-O from an aqueous solution. The optimal conditions for absorption provided at pH 7, an initial concentration of dye of 1.5 gr.L⁻¹, and an adsorbent dosage of 0.1 gr. Also, the optimal time for LN and LN/PAA hydrogel were 100 min and 450 min, respectively. Both adsorbent LN and LN/PAA hydrogel showed good agreement with the Langmuir isotherm. The maximum absorption capacities of LN and LN/PAA hydrogel were determined to be 100 mg.gr⁻¹ and 1666.6 mg.gr⁻¹, respectively. Both adsorbent LN and LN/PAA hydrogel follow the pseudo-second kinetic model and the intraparticle diffusion model.

Keywords: lignin, nanoparticles, ethylene glycol, polyacrylic acid, Safranin-O, hydrogel

INTRODUCTION

Safranin-O dye is highly soluble in water and is nonvolatile. It is red in color and is a cationic dye of the imine group. Safranin-O is dangerous and toxic [1].

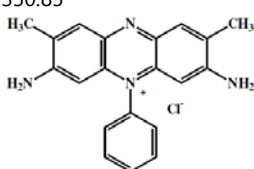
Adsorption processes are physical processes that have advantages compared to other waste technologies; they are low cost, accessible, and capable of treating dye in high concentrations. A variety of natural and synthetic adsorbents are used to bleach dyes; natural adsorbents are environmentally friendly, are low cost, have a high absorption capacity, lack toxicity, and cause few problems in the final desorption phase [2].

After cellulose, lignin is the second most abundant natural polymer; it consists of phenylpropane structural units with carbon-carbon and ether connections. Lignin is an amorphous and super complex structure that has yet to be fully investigated [3].

Hydrogels are three-dimensional structures with linear polymer chains that have covalent bonds. Nanocomposite hydrogels are network structures of hydrophilic homopolymers or copolymers. Some hydrogels are not used widely because of their low stability, high production cost, and toxicity. Therefore, the use of natural materials in nanocomposite hydrogel is very functional due to their easy operation, low power consumption, easy maintenance, high absorption capacity, and high performance [4]. Luo et al., in 2015, evaluated the chemical properties of nanocomposite hydrogels and prepared isopropyl acrylamide/alkali lignin [5]. In 2011, Ma et al. prepared a cellulose/acrylic acid copolymer by the copolymerization of radicals; the absorption capacity of methylene blue and the rate of swelling were determined to be 2,197 mg.gr⁻¹ and 7,32%, respectively [6].

The purpose of this research was to prepare LN/PAA hydrogel for the removal of Safranin-O. In addition, the pH, adsorbent dosage, dye concentration, and contact time were studied as factors in the absorption process. Further, pseudo-first order, pseudo-second order, and intraparticle diffusion were investigated in the Langmuir, Freundlich, and Temkin models to evaluate the absorption processes.

Table 1. Chemical and physical characteristics of the Safranin-O dye [7]

C.I. name	Safranin-O
C.I. number	50240
Common name	Basic red 2
Other name	Safranin-T, Basic red 2
Class	Safranin
Ionization	Basic
Aqueous solubility (%)	5.45
Colour	Red
Absorption maximum (nm)	517
Chemical formula	C ₂₀ H ₁₉ N ₄ Cl
Formula weight (g/mol)	350.85
structure	

MATERIALS AND METHODS

Materials

AL was prepared by the acidification of black liquor obtained from the Pars Khuzestan paper factory in Iran. Safranin-O dye (99.5%), sodium hydroxide (99%), hydrochloric acid (wt% 36), and ethylene glycol (98%), potassium persulfate, N,N'-Methylenebis(acrylamide) (98%), and acrylic acid purchased from Merck in Germany. Ethanol (99.9%) was prepared by Bidestan in Iran. The chemical structure and features of the Safranin-O dye are shown in [Table 1](#) [7].

Devices

Fourier transform infrared spectroscopy (FT-IR) was used to determine the chemical structures of the compounds in the range of 400 to 4,000 cm⁻¹ using a Tensor 27 FT-IR spectrophotometer made by Bruker in Germany. In order to determine the amount of dye absorption, Safranin-O dye was used. To determine the amount of ultraviolet-visible absorption, a Model M350 Double Beam Spectrophotometer was used (UK). The pH was determined using a Model Metrohm 827 pH meter. In order to study structural changes in the synthesis of compounds as well as heat resistance up to 500°C, a thermogravimetric analysis (TGA-DTG) device (Model Perkin Elmer) was used (UK). In addition, a Zetasizer PSS0012-22 (Malvern) made in USA was used for dynamic light scattering (DLS), and scanning electron microscope (SEM) device (Model LEO 1455VP) made in UK, was used in order to determine the particle size and morphology of the surface of the absorbent. Gel permeation chromatography (GPC) was performed with a Shimadzu 6-A made in USA, to determine the molecular weight of the AL.

Preparation of Alkali Lignin

To precipitate the AL, acidic black liquor from a pulp and paper factory in Khuzestan was placed in 0.1 N of hydrochloric acid in a pH range of 2.5–3. The impure lignin precipitate sediment was centrifuged and isolated. The sediment was washed with distilled water until the filter effluent reached a pH of about 7. In order to purify, lignin was dissolved in relatively warm ethanol (50–60°C). Ethanol-soluble fractions were separated by filtration, and the solid residue was discarded. The bulk of the ethanol (75%) in the evaporator was evaporated at low pressure. Distilled water was poured on the remaining solution and the sediment of lignin in a colloidal form [8]. The molecular weight (M_w) and polydispersity index (PDI) of the AL obtained 2530 gr.mol⁻¹ and 1.65, respectively, using gel permeation chromatography.

Preparation of Lignin Nanoparticles

AL (0.28 gr) was dissolved in 50 ml of polyethylene glycol (wt% 0.56) and was stirred for 2 h at a temperature of 40° C. Then, it was filtered with 0.4-µm filters for purification. Next, hydrochloric acid 0.25 M was slowly dropped in 45 ml of the filtered solution at a pH of 4. The Lignin nanoparticles were formed in this solution [9].

Safranin-O Dye Absorption

A stock solution with a concentration of 2 gr.L⁻¹ was prepared and maintained at a temperature of 4°C. All experiments were carried out with 100 ml of dye at a temperature of 25°C on a shaker at 70 rpm. The samples were filtered after each step to measure the concentration of the dye, and the absorption rate was determined using ultraviolet-visible absorption spectroscopy at a wavelength of 517 nm. Each sample was tested three times, and the averages were recorded. The amount of dye adsorbed at equilibrium (q_e (mg.gr⁻¹)) and the dye removal efficiency (R%) were determined using equations (1) and (2), respectively [11].

$$q_e = (C_0 - C_e)V/M \quad (1)$$

$$\%R = 100(C_0 - C_e)/C_0 \quad (2)$$

C_0 and C_e represent the initial and final concentrations of dye in the solution (mg.L⁻¹), respectively, V is the volume of the solution (L), M is the adsorbent mass (gr), and q_e is the amount of dye adsorbed at equilibrium (mg.gr⁻¹).

Isoelectric Range

The point zero charge (pH_{pzc}) characteristic of LN and LN/PAA hydrogel was determined using the solid addition method [12]. The experiment was conducted in a series of 100 mL flasks with glass-stoppered. Each flask was filled with 20 mL of potassium nitrate 0.1M solutions of different initial Ph values (pH_0) and 0.20 g of LN or LN/PAA hydrogel. The pH values of the KNO₃ solutions were adjusted 2-10 with sodium hydroxide 0.1M and diluted hydrochloric acid. The suspensions were then sealed and shaken for 24h at 100 rpm and 24°C. The final Ph values (pH_f) of the supernatant liquid were noted. The difference $\Delta pH(pH_0 - pH_f)$ between the initial and final pH values was plotted against pH_0 . The point of intersection of the resulting curve with the abscissa gave the pH_{pzc} .

RESULTS

Determining Lignin Nanoparticle Size Using Dynamic Light Scattering

The particle size distribution of lignin nanoparticles at a pH of 4, as a function of the percentage of nanoparticles, is presented in [Figure 1](#). The LN size at a pH of 4 was estimated to be between 40 nm and 60 nm, and the average diameter of the nanoparticles was determined to be 52.7 nm.

Morphology of Alkali Lignin and Lignin Nanoparticles

In order to study the morphology and approximate particle size of AL, LN and LN/PAA hydrogel, a scanning electron microscope was used. The AL and LN morphologies, before and after the adsorption of Safranin-O, are shown in [Figure 2](#). AL macromolecules have homogeneous and interconnected particles that are relatively uniform and flat. LN have an average diameter of less than 80 nm and highly porous surfaces. The matrix surface has a honeycomb structure with a relatively uniform dispersion.

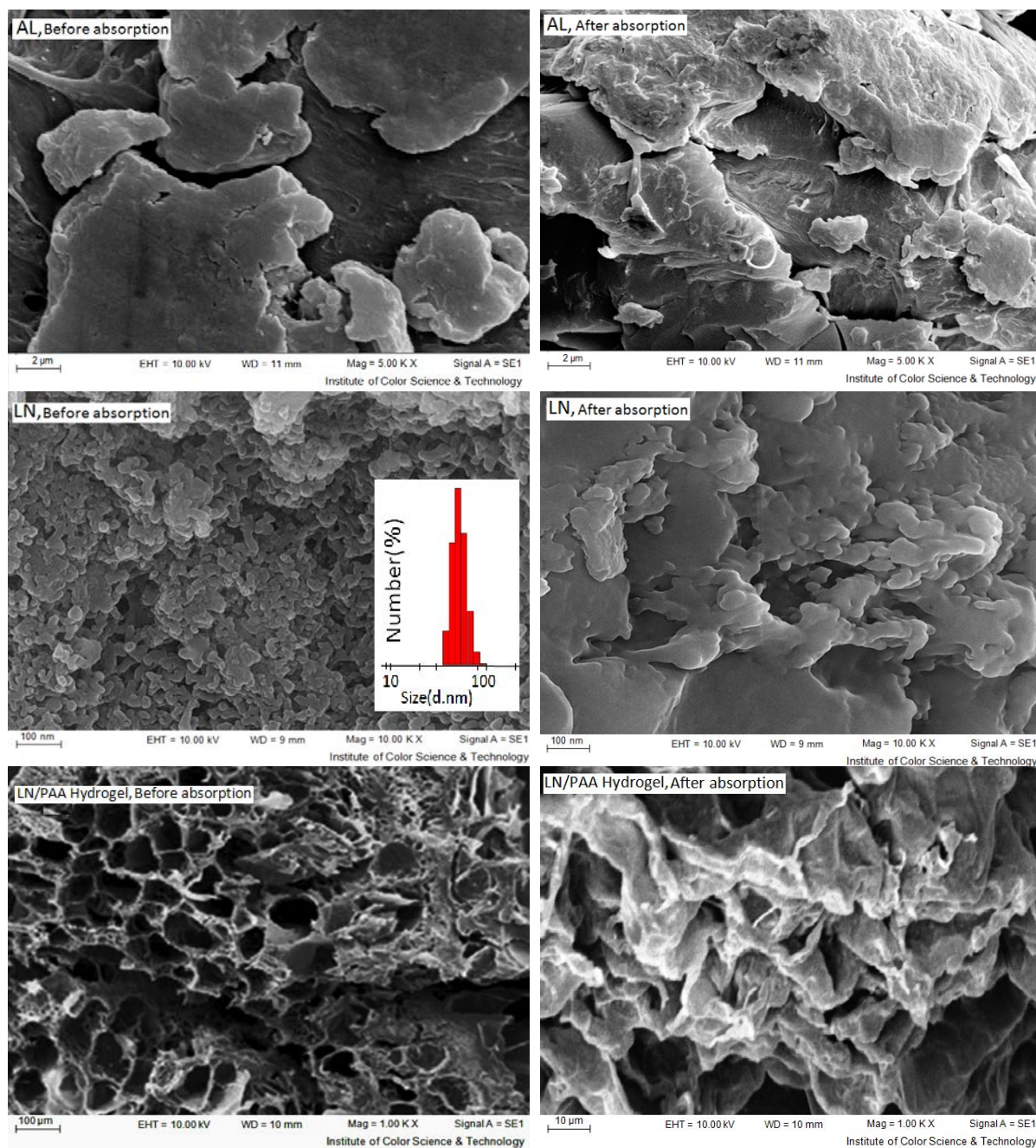


Figure 2. SEM images of AL, LN and LN/PAA hydrogel before and after the absorption of Safranin-O dye

FT-IR Spectra

The FT-IR spectra of PAA, AL, LN, and LN/PAA hydrogel are shown in [Figure 3](#). The FT-IR spectra of AL and LN are very similar to each other. No change was seen in the chemical structure of AL in the process of creating nanoparticles. The weak peak at $1,709\text{ cm}^{-1}$ shows the good vibration of Carbonyl bonds in the carboxylic acid groups. The peak at $1,315\text{ cm}^{-1}$ in the LN shows the stretching vibration in connecting syringyl (S) and guaiacyl (G), which occurred as a result of nanoparticles formation. In AL compound, the peak at the $3,405\text{ cm}^{-1}$ area relates to the vibration of -OH bonds, which, in LN compound due to connection with the ethylene glycol, moved to $3,394\text{ cm}^{-1}$ and increased in intensity. The stretching vibration of amide carbonyl groups in the $1,628\text{ cm}^{-1}$ area indicates the presence of crosslinking N,N'-methylene-bisacrylamide in the LN/PAA hydrogel. In the LN/PAA hydrogel, the carbonyl group in the carboxylic acid transferred from the $1,709\text{ cm}^{-1}$ area to the $1,716\text{ cm}^{-1}$ area as a result of copolymerization. Thus, PAA chains containing carboxylic acid groups was network to LN in the LN/PAA hydrogel.

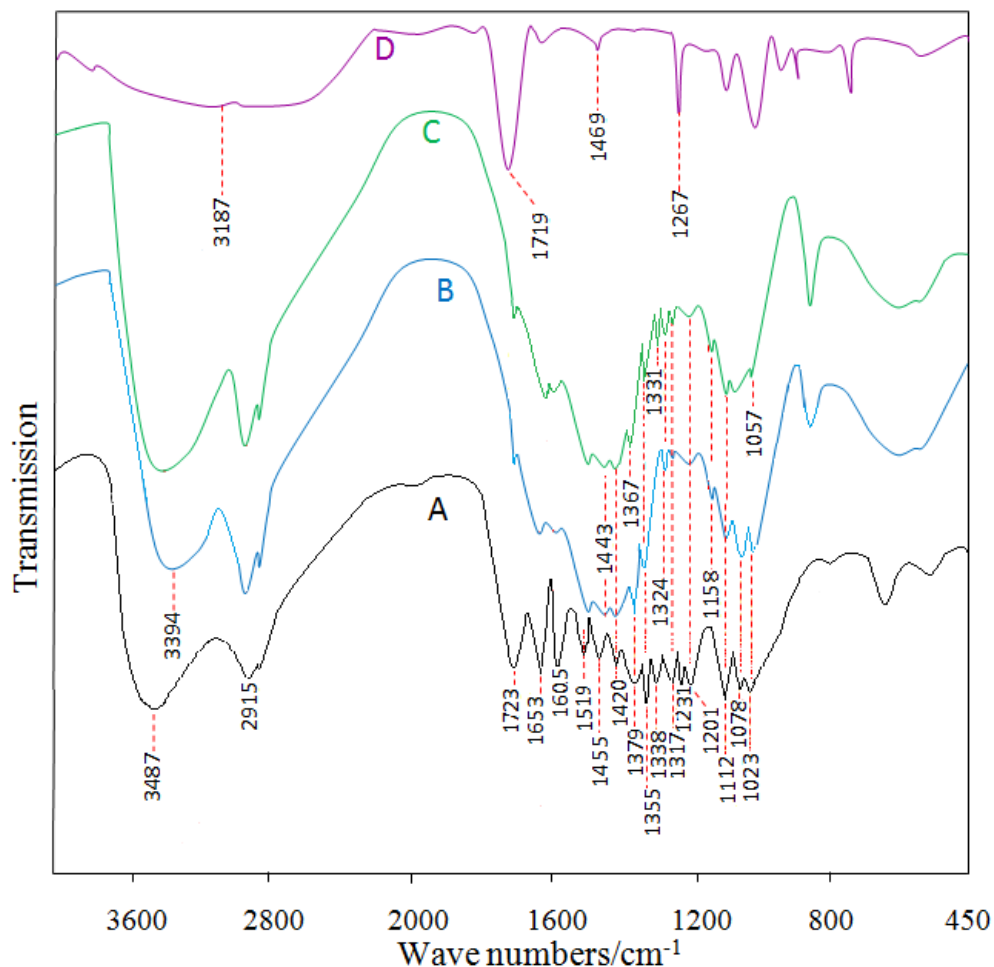


Figure 3. FT-IR spectra of LN/PAA hydrogel (A), LN (B), AL (C) and PAA(D)

Thermal Stability

The thermogravimetric analysis (TGA) and differential thermogravimetric (DTG) spectra of PAA, LN and LN/PAA hydrogel are shown in **Figure 4**. The weight loss of LN occurred in two stages. The first was attributed to the evaporation of water and the second, which was attributed to the breaking of the syringyl, guaiacyl, and p-hydroxyphenyl polymer units in the LN. But weight loss in the PAA samples and LN/PAA hydrogel was done in three stages. The first, which was attributed to the evaporation of water contained in the compounds. The second, which was attributed to the decomposition of carboxylic acids and breaking of the crosslinker in the hydrogel. Also, The third, which was attributed to the breaking of the main chain in the PAA and breaking of the syringyl, guaiacyl, and p-hydroxyphenyl polymer units in the LN/PAA hydrogel.

In the LN/PAA hydrogel, increasing the temperature to 341°C resulted in the carboxylic acid groups in the PAA breaking and crosslinker bond decomposition, preventing heat transfer to the main structure of the LN. Break the main chains in the LN and LN/PAA hydrogel begins at temperature 146°C and 341°C, respectively, which has increased 195°C in the LN/PAA hydrogel. The results show more structural changes in the LN/PAA hydrogel compared to in the LN due to copolymerization with polyacrylic acid and crosslinking formation.

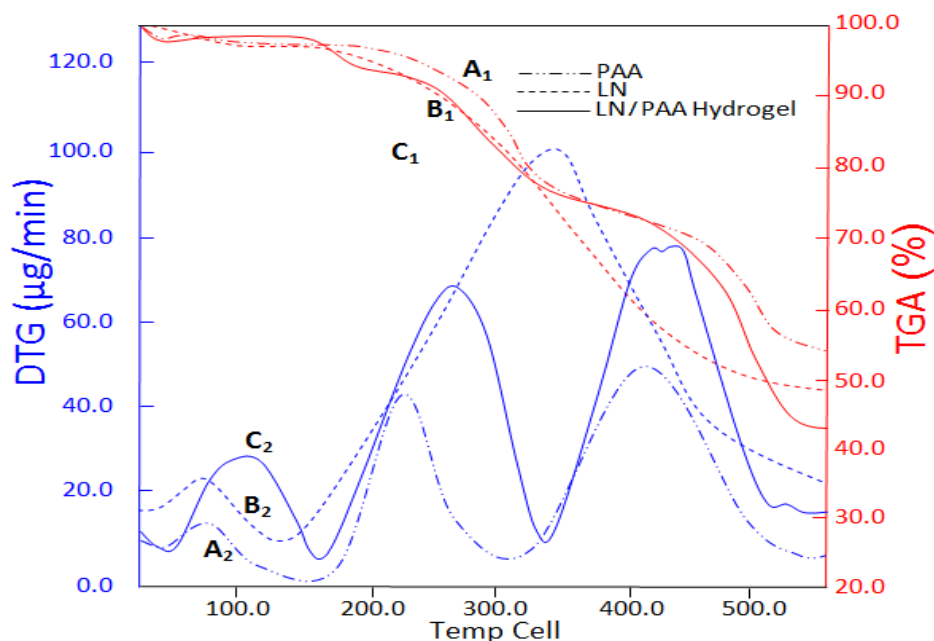


Figure 4. TGA and DTG curves in the PAA (A₁ and A₂), LN (B₁ and B₂) and LN/PAA hydrogel (C₁ and C₂)

Factors that Affect Absorption

Effect of initial pH

The optimal pH was investigated. According to the stability of LN/PAA hydrogel, the absorption of Safranin-O dye was evaluated at a pH range of 3–10.

The isoelectric points (pH_{PZC}) of the LN and LN/PAA hydrogel were 5.6 and 5.5, respectively. The pH_{PZC} decrease in the LN/PAA hydrogel was attributed to the increased K_a in the AA monomers; as a result, acidic hydrogen released in a lower pH. A decrease in pH from pH_{PZC} to 2 reduced the absorption capacity and the percentage of dye removal; this is because, by reducing the pH, the concentration of H^+ increased, so many $-NH_2$ functional groups were protonated on the dyes quantitatively and were unable to create hydrogen bonds.

At pH_{PZC} , the compounds had no electric charge; however, at $pH > pH_{PZC}$, the electrical charge was negative due to the loss of acidic hydrogen in the carboxylic acid groups of the LN and LN/PAA hydrogel. By introducing electrostatic attraction with the Safranin-O dye, the absorption capacity and percentage of dye removal increased. In a pH range of 5–6, the adsorption capacity and percentage of dye removal increased dramatically. The adsorption capacities of LN and LN/PAA hydrogel at a pH of 7 were 90 $mg \cdot g^{-1}$ and 941 $mg \cdot g^{-1}$, respectively. The adsorption data at a pH of 10 demonstrates the significant effect of carboxylic acid groups on the creation of electrostatic attraction in the process of absorption.

Effect of adsorbent dosage

The effect of adsorbent dosage on the adsorption of Safranin-O dye was investigated. By increasing the amount of adsorbent, the absorption capacity reduced slightly; this is because, with low amounts of adsorbent, there is more competition between dye molecules to connect to the adsorbent. Thus, the adsorption capacities of the LN and LN/PAA hydrogel in the use of 0.02 gr of adsorbent were 210 $mg \cdot g^{-1}$ and 1320 $mg \cdot g^{-1}$, respectively. By increasing the amount of adsorbent to 0.1 gr, the adsorption capacities of the LN and LN/PAA hydrogel reduced to 91.9 $mg \cdot g^{-1}$ and 995 $mg \cdot g^{-1}$, respectively.

Effect of contact time

The effect of contact time on Safranin-O dye absorption was evaluated. The adsorption capacity and percentage of Safranin-O dye removal for both LN and LN/PAA hydrogel was initially rapid; after about 100 min for LN Compound and 450 min for LN/PAA hydrogel, they reached equilibrium and remained almost constant. Therefore, the optimal times for LN and LN/PAA hydrogel were determined to be 100 min and 225 min,

Table 2. Effect of the Langmuir isotherm, Freundlich isotherm, and Temkin isotherm on Safranin-O dye adsorption (dye concentration = 1.5 gr.L⁻¹, pH = 7, adsorbent dose = 0.1 gr, contact time = 100 min (for LN) and 450 min (for LN/PAA hydrogel))

Absorbent type	Temp (°C)	Langmuir isotherm			Freundlich isotherm				Temkin isotherm			
		R ²	q _{e max} (mg.gr ⁻¹)	K _L (L.gr ⁻¹)	R _L	R ²	1/n	n	K _F (L.mg ⁻¹)	R ²	B _t	K _t
LN	2±25	0.999	100	0.012	0.052	0.68	0.11	8.96	40.52	0.69	9.2	14.29
LN/PAA Hydrogel		0.981	1666.6	0.0001	0.87	0.68	0.131	7.51	627.09	0.78	169.8	13.06

respectively. At optimal time, the removal capacities of LN and LN/PAA hydrogel were 99.2 mg.g⁻¹ and 1060 mg.g⁻¹, respectively.

Effect of initial dye concentration

The effect of initial dye concentration on the absorption capacity and percentage of dye removal was investigated using adsorbent LN and LN/PAA hydrogel. With increased initial dye concentrations, a greater amount of dye interacts with the surface of the adsorbent, thereby increasing the absorption capacity. The absorption capacities, at a maximum concentration of 1.5 gr.L⁻¹ of LN and LN/PAA hydrogel adsorbent, were 91.9 mg.g⁻¹ and 1060 mg.g⁻¹, respectively.

Adsorption Isotherms

Adsorption isotherms provide equations to describe the adsorption equilibrium between solid and fluid phases. The Langmuir and Freundlich equations are shown in equations (3) and (4), respectively [13].

$$\frac{C_e}{q_e} = 1/(q_{max} \cdot K_L) + \left(\frac{C_e}{q_{max}}\right) \tag{3}$$

$$\ln q_e = \ln K_F + 1/n(\ln C_e) \tag{4}$$

K_L(L.gr⁻¹) represents the Langmuir isotherm constant, q_{max} (mg.gr⁻¹) is the maximum absorption capacity, n and K_F(mg.L⁻¹) are Freundlich isotherm constants, and C_e(mg.L⁻¹) is the concentration of adsorbates, after reaching equilibrium in the liquid phase and the q_e (mg.gr⁻¹) amount of adsorbates in the unit mass of the adsorbent. K_F represents the absorption capacity, and 1/n represents the adsorption intensity.

An essential characteristic of the Langmuir isotherm is a constant and dimensionless parameter called R_L, which can be obtained from equation (5) [13].

$$R_L = 1/(1 + K_L \cdot C_0) \tag{5}$$

C₀ (mg.L⁻¹) represents the initial dye concentration in the solution.

The Temkin isotherm is linear and can be determined by equation (6) [13].

$$q_e = B_t \ln K_t + B_t \ln C_e \tag{6}$$

Using the curve q_e in Ln C_e, B_t and K_t were determined by the slope and intercept of the curve.

Evaluation of the Langmuir, Freundlich, and Temkin Isotherm Models

The Langmuir, Freundlich, and Temkin isotherm models were examined, and their data are shown in Table 2. The R_L data in the Langmuir model and 1/n in the Freundlich model for both the LN and LN/PAA adsorbents are between 0 and 1; the Safranin-O dye absorption of both the LN and LN/PAA hydrogel was assessed desirable using the Langmuir and Freundlich models. The R₂ greater in the both the LN and LN/PAA hydrogel showed dye absorption followed of the Langmuir isotherm. The maximum adsorption capacity of LN was 100 mg.gr⁻¹ and that of LN/PAA hydrogel was 1666.6 mg.gr⁻¹ in the Langmuir model, both of which are close to the experimental values. The high absorption capacity of the LN/PAA hydrogel was attributed to the quantitative increase in carboxylic acid groups in the polymer chain of the AA connected to the phenoxy radicals in the LN during polymerization.

Absorption Kinetics

Absorption kinetics were studied to determine the factors that influence the rate of absorption. The linear pseudo-first-order kinetic model is shown in equation (7) [14].

$$\ln(q_e - q_t) = \ln(q_e) - (K_1 t) \tag{7}$$

Table 3. Pseudo-first-order, pseudo-second-order, and intraparticle diffusion kinetic models for BR2 dye adsorption (dye concentration = 1.5 gr.L⁻¹, pH = 7, adsorbent dose = 0.1 gr, contact time = 100 min (for LN) and 450 min (for LN/PAA hydrogel))

Absorbent type	Temp (°C)	(q _e) _{Exp} (mg.gr ⁻¹)	Pseudo-first-order model			Pseudo-second-order model			intraparticle diffusion model		
			R ²	(q _e) _{Cal} (mg.gr ⁻¹)	K ₁ (min ⁻¹)	R ²	(q _e) _{Cal} (mg.gr ⁻¹)	K ₂ (min ⁻¹)	R ²	K _p	C
LN		92	0.84	42.5	0.033	0.999	99	0.0012	0.99	3.2	60.13
LN/PAA Hydrogel	2±25	1060	0.86	601.8	0.005	0.992	909.09	0.000057	0.97	21.7	512.29

q_e (mg.gr⁻¹) represents the amount of dye adsorbed at equilibrium, q_t (mg.gr⁻¹) shows the amount of dye adsorbed at time t, and K₁(min⁻¹) represents constant first-order kinetics at equilibrium.

The linear pseudo-second-order kinetic model is shown in equation (8) [14].

$$\frac{t}{q_t} = \frac{1}{k_2 \cdot q_e^2} + \left(\frac{t}{q_e}\right) \quad (8)$$

K₂(gr.mg⁻¹.min⁻¹) represents constant first-order kinetics at equilibrium.

The intraparticle diffusion model is presented in equation 9 [14].

$$q_t = K_p \cdot t^{1/2} + C \quad (9)$$

K_p (mg.gr⁻¹.min^{-1/2}) is the intraparticle diffusion constant and C (mg.gr⁻¹) Intraparticle diffusion constant. Using the curve q_t in t^{1/2}, K_p and C were determined.

Evaluation of pseudo-first-order, pseudo-second-order, and intraparticle diffusion kinetic models

K, q_e and R² in the pseudo-first-order and pseudo-second-order kinetic models and K_p and C in the intraparticle diffusion model were examined, and their data are shown in **Table 3**. The correlation coefficients (R₂) in the pseudo-second-order and intraparticle diffusion kinetic models are similar and are greater than the correlation coefficient in the pseudo-first-order kinetic model. Therefore, the bleaching process can be described by both pseudo-second-order and intraparticle diffusion models.

In the pseudo-second-order kinetic model, the absorption capacities of LN and LN/PAA hydrogel were 99 mg.gr⁻¹ and 909.09 mg.gr⁻¹, respectively, in the computational results and 92 mg.gr⁻¹ and 1060 mg.gr⁻¹, respectively, in the experimental results. The proximity of the experimental and theoretical results show that the pseudo-second-order kinetic model is appropriate to determine Safranin-O dye adsorption in LN and LN/PAA hydrogel.

CONCLUSION

This study was conducted to assess the efficacy of LN/PAA hydrogel Nanocomposites as cheap Superabsorbent that are environmentally friendly in the removal of cationic Safranin-O from aqueous solutions. The results showed that the absorption capacity in LN/PAA hydrogel increased than the LN to almost 16.5-fold. Adding polar groups of -COOH to the structure of natural absorbents is an effective method to absorb Safranin-O dye; by increasing electrostatic attraction and hydrogen bonding, the absorption capacity and percentage of dye removal also increase.

Absorption using pseudo-second-order and intraparticle diffusion kinetic models for LN and LN/PAA hydrogel absorbents occurs according to the principles of two-stage absorption kinetics. In the first stage, the dye removal rate is increased by adsorption; in the second stage, the dye removal rate is decreased due to the influence of the porous surface.

Thus, LN/PAA hydrogel achieved a suitable absorption capacity and compatibility with the environment; thus, they are suitable for the removal of wastewater containing Safranin-O dye.

REFERENCES

- Gong R, Li M, Yang C, Sun Y, Chen J. Removal of cationic dyes from aqueous solution by adsorption on peanut hull. *Journal of Hazardous Materials*. 2005;121(1-3):247-50. <https://doi.org/10.1016/j.jhazmat.2005.01.029>
- Mohan D, Singh KP, Singh G, Singh G, Kumar K. Removal of Dyes from Wastewater Using Flyash, a Low-Cost Adsorbent. *Ind. Eng. Chem. Res.* 2002;41(15):3688-95. <https://doi.org/10.1021/ie010667>

3. Hu S, Hsieh YL. Synthesis of surface bound silver nanoparticles on cellulose fibers using lignin as multi-functional agent. *Carbohydrate Polymers*. 2015;131:134-41. <https://doi.org/10.1016/j.carbpol.2015.05.060>
4. Lee WF, Yang LG. Superabsorbent polymeric materials. XII. Effect of montmorillonite on water absorbency for poly(sodium acrylate) and montmorillonite nanocomposite superabsorbents. *J. Appl. Polym. Sci.* 2004;92(5):3422-9. <https://doi.org/10.1002/app.20370>
5. Luo H, Ren S, Ma Y, Fang G, Jiang G. Preparation and properties of kraft lignin-N-isopropyl acrylamide hydrogel. *Bio Resources*. 2015;10(2):3507-19. <https://doi.org/10.15376/biores.10.2>
6. Zhou Y, Fu S, Liu H, Zhan H. Removal of methylene blue dyes from wastewater using cellulose-based superadsorbent hydrogels. *Polymer Engineering & Science*. 2011;51(12):2417-24. <https://doi.org/10.1002/pen.22020>
7. Sun XF, Ye Q, Jing Z, Li Y. Preparation of hemicellulose-g-poly(methacrylic acid)/carbon nanotube composite hydrogel and adsorption properties. *Polymer Composites*. 2014;35(1):45-52. <https://doi.org/10.1002/pc.22632>
8. Gupta, AK, Mohanty S, Nayak SK. Synthesis, Characterization and Application of Lignin Nanoparticles (LNPs). *Materials Focus*. 2014;3(6):444-454. <https://doi.org/10.1166/mat.2014.1217>
9. Frangville C, Rutkevicius M, Richter AP, Velev OD, Stoyanov SD, Paunov VN. Fabrication of Environmentally Biodegradable Lignin Nanoparticles. *ChempHyschem*. 2012;13(18):4235-43. <https://doi.org/10.1002/cphc.201200537>
10. Sun Y, Ma Y, Fang G, Li S, Fu Y. Synthesis of Acid Hydrolysis Lignin-g-Poly-(Acrylic Acid) Hydrogel Superabsorbent Composites and Adsorption of Lead Ions. *BioResources*. 2016;11(3):5731-42. <https://doi.org/10.15376/biores.11.3>
11. Fanchiang J-M, Tseng D-H. Degradation of anthraquinone dye C.I. Reactive Blue 19 in aqueous solution by ozonation. *Chemosphere*. 2009;77(2):214-21. <https://doi.org/10.1016/j.chemosphere.2009.07.038>
12. Tang Y, Zeng Y, Hua T, Zhou Q, Peng Y. Preparation of lignin sulfonate-based mesoporous materials for adsorbing malachite green from aqueous solution. *Journal of Environmental Chemical Engineering*. 2016;4(3):2900-10. <https://doi.org/10.1016/j.jece.2016.05.040>
13. Niu Y, Qu R, Sun C, Wang C, Chen H, Ji C, Zhang Y, Shao X, Bu F. Adsorption of Pb(II) from aqueous solution by silica-gel supported hyperbranched polyamidoamine dendrimers. *Journal of Hazardous Materials*. 2013;244-245C:276-86. <https://doi.org/10.1016/j.jhazmat.2012.11.042>
14. Gil A, Assis FCC, Albeniz S, Korili SA. Removal of dyes from wastewaters by adsorption on pillared clays. *Chemical Engineering Journal*. 2011;168(3):1032-40. <https://doi.org/10.1016/j.cej.2011.01.078>

<http://www.eurasianjournals.com>